The effect of mesh resolution on the calculated cogging torque of permanent magnet motors

Gergely Máté Kiss

Budapest University of Technology and Economics, Department of Electric Power Engineering
1111 Budapest, Egry J. u. 18., V1. épület, III-IV. em
email: kiss.gergely@vet.bme.hu

István Vajda

Obuda University, Institute of Automation
1034 Budapest, Bécsi út 94-96.
email: vajda@uni-obuda.hu

Abstract: The initial sizing of permanent magnet synchronous machines for general power and torque can be carried out using simple analytical methods. Low complexity finite element models can be used to control the calculation and refine the results. Fine parameters of the motor like cogging torque however are difficult to predict with high accuracy. This is especially true for machines designed with saturated magnetic circuit. Cogging has a nonlinear behavior and may vary significantly even if the input parameters undergo very small changes. The resolution of the finite element model's mesh is one these parameters. This study will investigate how the calculated cogging torque of a permanent magnet machine depends on the finite element mesh

Keywords: cogging torque, permanent magnet synchronous motor, simulation, mesh, finite element method

1. Introduction

Permanent magnet synchronous motors (PMSM) have a couple of advantage that make them the favored motor type for more and more applications. They can be designed for high power densities which makes them suitable for products with a mass limit e.g. motors in drones and electric motor assisted gliders and planes but also for products which require high power for short periods of time e.g. servo drives, motor assisted vehicles. PMSM drives utilize electronic commutation which ensures a long lifetime due to the reduced mechanical wear. They are relatively easy to control both for speed and torque with basic drive units therefore the motor dynamics can be adjusted as required. When the use of a rotor position sensor is not an option PMSM drives can also be implemented in sensor-less control.

One major drawback however is that they have an undesired cogging torque, due to the interaction of the rotor magnets and the stator slotting. Its reduction is commonly a design objective since it is often related to user discomfort and elevated noise levels. [1] Therefore this specific property of the PMSM is usually treated with special care.

Finite element method (FEM) is often utilized to obtain a machine design's torque waveform since a pure analytical calculation might be limited by geometry. The goal of the FEM analysis is usually to forecast the cogging torque waveform of a design and support the optimization of the geometry for a preferably minimal cogging torque. These goals require the modeling method to be reliable, precise and fast at the same time, since the optimization process usually needs several iterations to complete.

There are numerous techniques to reduce the time required for solving the FEM model on a given hardware e.g. taking advantage of symmetries, simplifying the geometry and of course choosing an appropriate finite element mesh resolution. The resolution of the mesh may have a significant effect on the calculated cogging torque, since cogging is greatly influenced by changes in geometry. Depending on the mesh resolution the calculated cogging of an electrical machine may change significantly. However the sensitivity of the model is design dependent, which means it is influenced by the geometry and materials.

2. Materials and Methods

This study uses two very similar motor models to demonstrate the calculated cogging torque's sensitivity to mesh resolution. They have the same overall dimensions and materials but have slightly different poles shape. The design parameters are described in Table 1 and an overview is presented in Fig. 1.

Table 1
Model parameters

Parameter	**Value**
Motor type	IPM spoke magnet
Phase number	3
Topology	10 pole, 30 slot
Rotor diameter	39 mm
Stator diameter	60 mm
Air gap	0.5 mm
Active length	20 mm
Stacking factor	95%
Core material	35-M235
Magnet material	NdFeB
Magnet coercivity	500 000 A/m

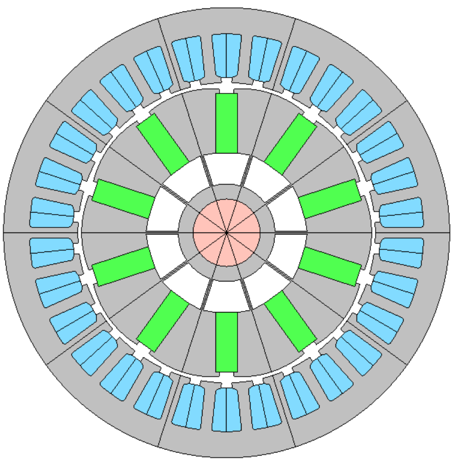

Figure 1

Overview of the motor with symmetry lines

2.1. The FEM Models

To reduce computation cost, the simulation is carried out for a 20th model for both models: Motor 1 (Fig. 2) and Motor 2 (Fig. 3).

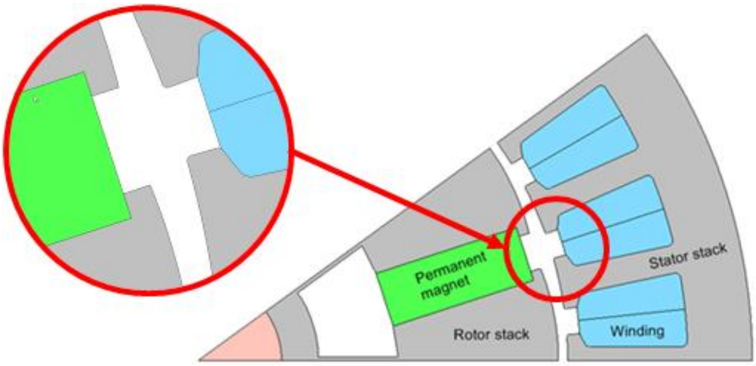

Figure 2

20th model for FEM simulation, 36° slice of the whole motor (Motor 1) demonstrating the pole shape

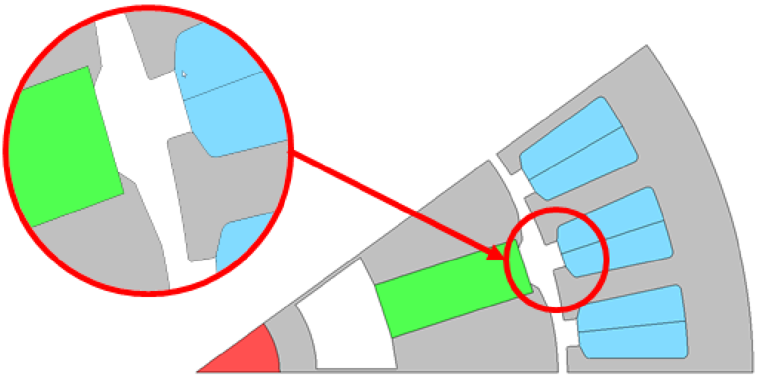

Figure 3

20th model for FEM simulation, 36° slice of the whole motor (Motor 2) demonstrating the pole shape

Exploiting model symmetries of course has drawbacks e.g does not allow the investiagtion of non-symmetric effects as manufacturing errors, individual pole or tooth damage, eccentricity and other misalignments.

However the goal of this study is to show the effect of mesh size and distibution on the outcome of the simulation. For this a set of mesh parameters are chosen and are varied within a given range. These parameters are:

- *Overall element size:* the global element size of the model
- *Radial divisions of the air gap:* number of layers of air in the gap
- *Angular divisions of the air gap:* number of elements along air gap in circumferential direction

The investigated values of these parameters are listed in Table 2.

Table 2
The list of investigated mesh parameters and their values

Parameter	**Value**
Overall element size [mm]	[10, 8, 6, 5, 2.5, 1, 0.75, 0.5, … 0.35, 0.25, 0.1, 0.05]
Radial division of air gap	[4, 8, 16]
Angular divisions of the air gap	[36, 72, 144]

A total of 56 were used out of the theoretically possible 108 cases, which would have been the full factorial approach. The selected value combinations represent the extrema of each set with a center point between them. Un-meshable models e.g. ones with very large global element size and high resolution gap and ones with very small global element size and low resolution gap mesh are also sorted out of the study.

The study aims to investigate extreme cases, therefore a wide range of mesh resolutions are simulated. The lowest resolution model is simulated with ~600 elements, and the highest resolution model has over 260.000 elements in its mesh. Figure 4 demonstrate the number of finite elements in the model for each case while Figures 5 to 6 give an overview of the meshed models.

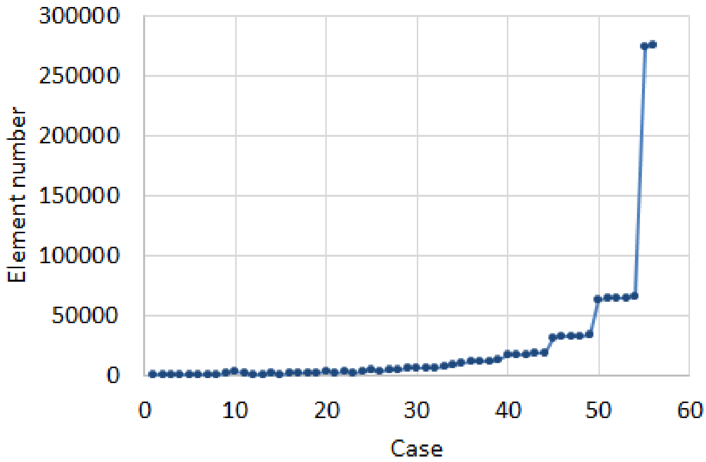

Figure 4

Number of finite elements in the model for each case

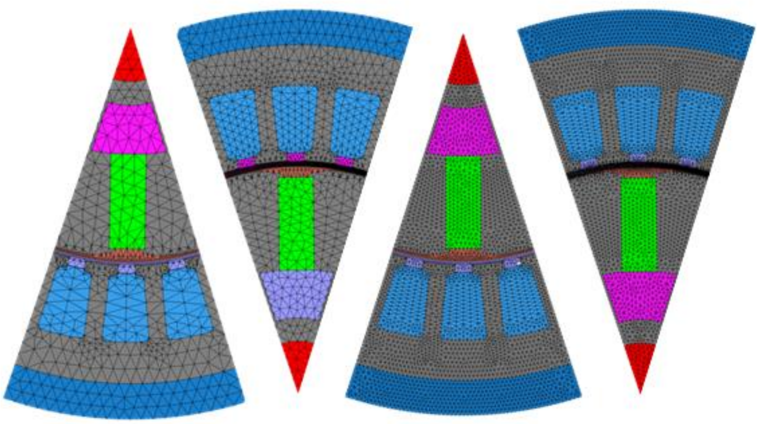

Figure 5

Overview of the mesh - 1

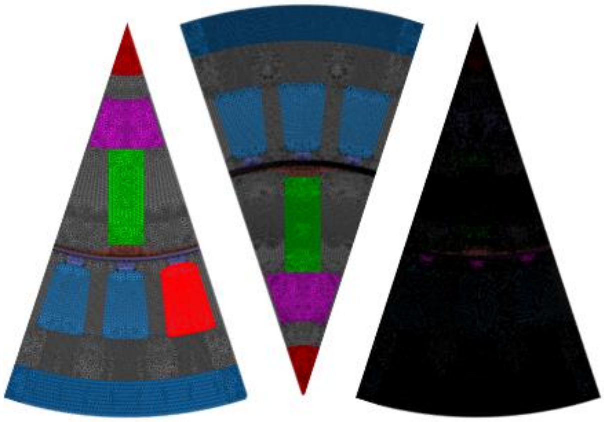

Figure 6

Overview of the mesh - 2

2.2. Simulation Setup

Based on the topology, the fundamental cogging torque order can be determined. The fundamental (natural) cogging torque harmonic is the least common multiple (LCM) of the pole number (p = 10) and the slot number (q = 30).

$$\nu_{fund.order} = \nu_{H1} = LCM(p,q) = 30 \tag{1}$$

Knowing the investigated harmonic's order its angular period in mechanical degrees can be determined.

$$\vartheta_{fund.order} = \vartheta_{H1} = 360° / \nu_{fund.order} = 12° \tag{2}$$

According to the Nyquist-Shannon sampling theorem an angular step size of less than 6° is required to get an accurate representation of cogging torque signal's fundamental.

Since harmonics are also interesting for this study a step size of 1° is chosen enabling the analysis of cogging torque harmonics from order 0. (DC component) up to the 5th harmonic of the fundamental.

The model is only solved for a partial rotation that is the period of the fundamental cogging torque order (12°). This results in limited spectral resolution of 30 order steps, so the simulation's outcomes will be following cogging torque harmonics:

$$\nu_{H0,H1,\ldots H5} = \{0,30,60,90,120,150\} \tag{3}$$

3. Results

The simulation of both motor models is carried out for all cases. The refercence case is chosen to be one with the highest mesh density (Case 56), since it can be assumed to be most precise model.

The flux density plots of Motor 1 and 2 are shown in Figure 7 and 8 respectively.

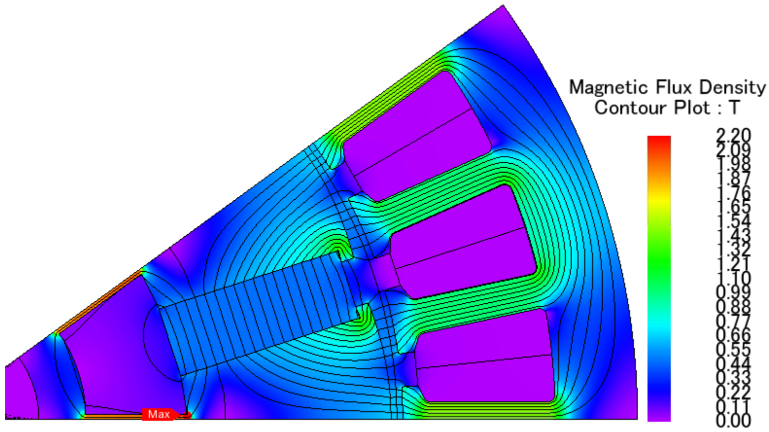

Figure 7

Flux density plot of Motor 1

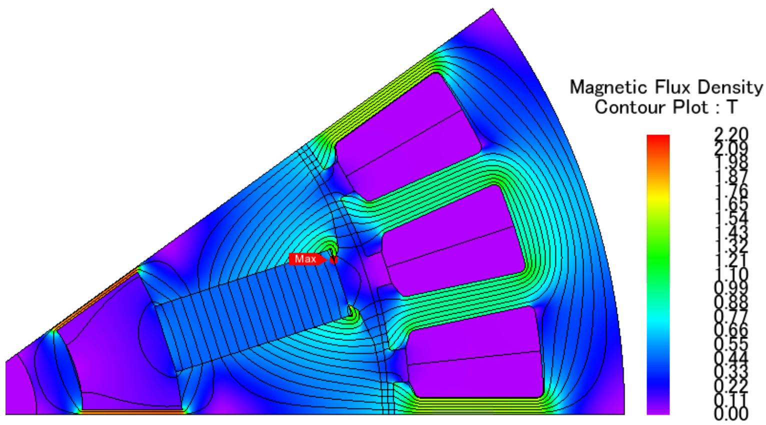

Figure 8

Flux density plot of Motor 2

It is worth noticing how the peak flux density values remain constant no matter the change of pole shape. However the slight change of pole shape influenced the flux density near the pole (of course) and in the teeth. In case of Motor 2 less flux loops around in the middle two teeth. Figure 9 gives a detailed view on the differences between the two models.

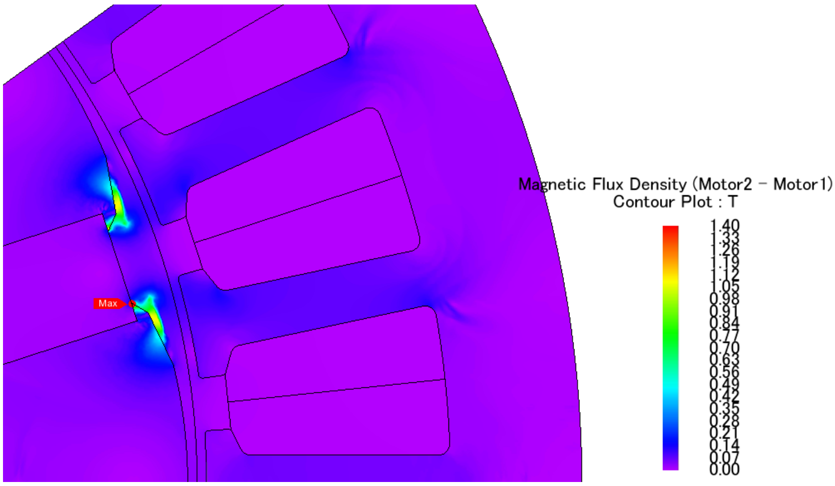

Figure 9

Flux density absolute difference plot of Motor 2 – Motor 1

3.1. Comparison of Reference Models

The induced voltage and cogging torque results of the reference case (Case 56) of Motor 1 are presented on Figures 10 to 13.

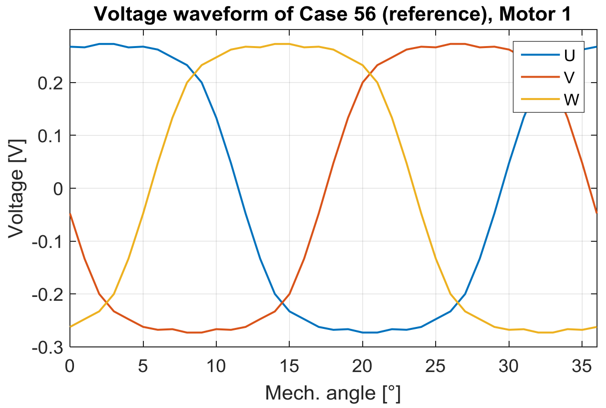

Figure 10

Induced voltage waveform of all phases, @1200 rpm speed, Motor 1

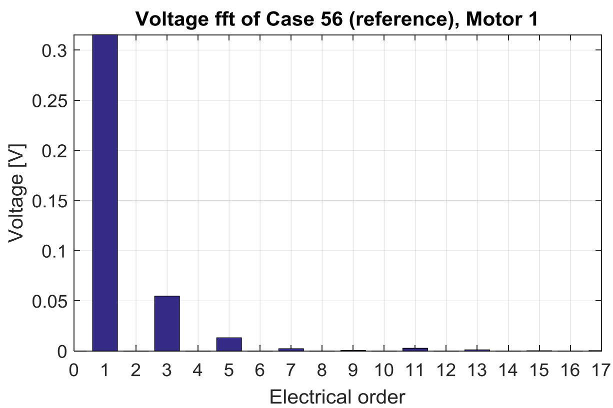

Figure 11

Induced voltage spectrum of phase U, @1200 rpm speed, Motor 1

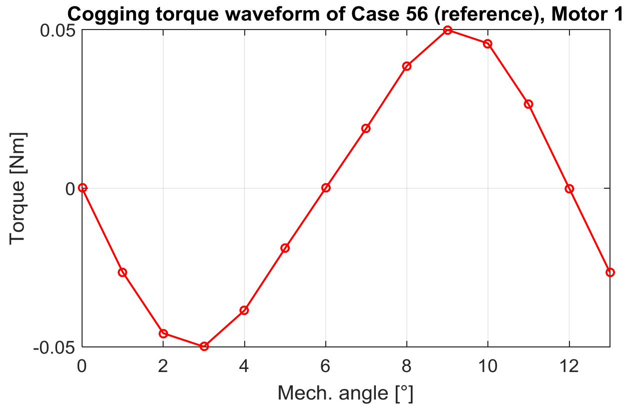

Figure 12

Cogging torque waveform, Motor 1

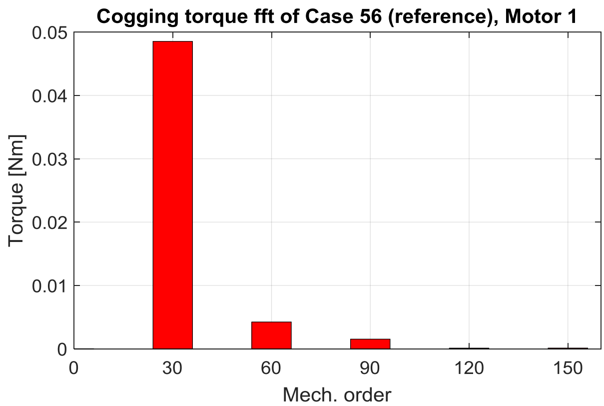

Figure 13

Cogging torque spectrum, Motor 1

The induced voltage and cogging torque results of the reference case (Case 56) of Motor 2 are presented on Figures 14 to 17.

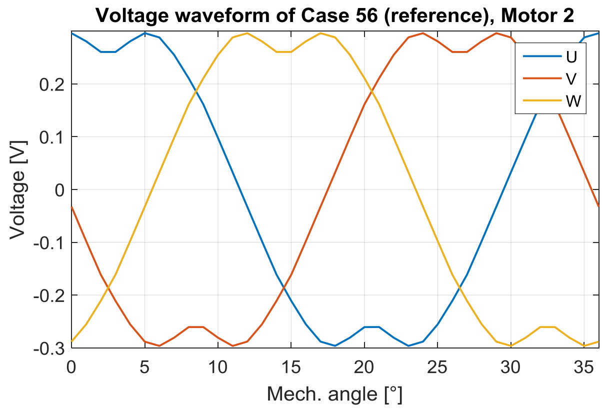

Figure 14

Induced voltage waveform of all phases, @1200 rpm speed, Motor 2

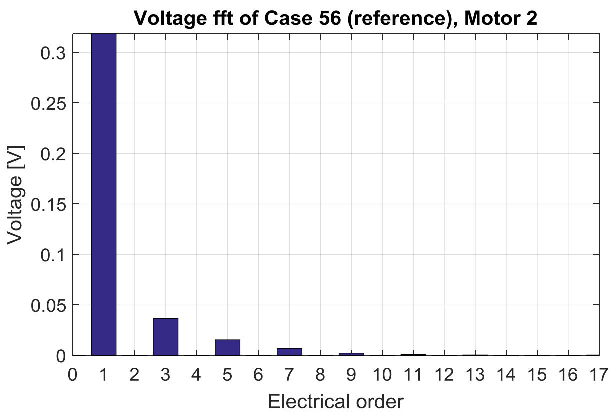

Figure 15

Induced voltage spectrum of phase U, @1200 rpm speed, Motor 2

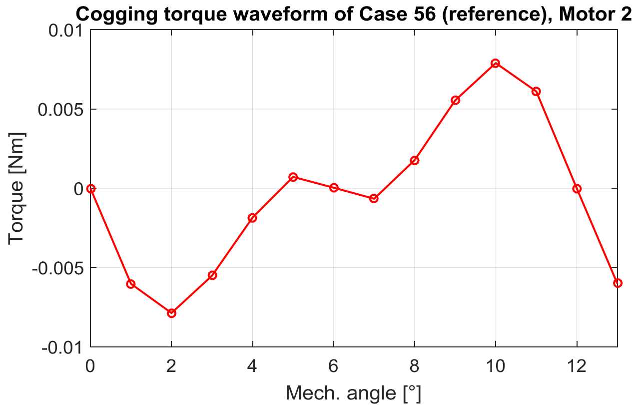

Figure 16

Cogging torque waveform, Motor 2

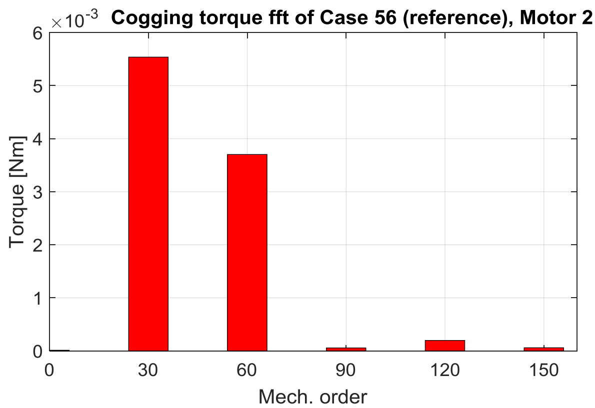

Figure 17

Cogging torque spectrum, Motor 2

Comparing the voltage and cogging values give a better overview on how Motor 1 and 2 are different from each other. The comparison is presented on Figures 18 – 21.

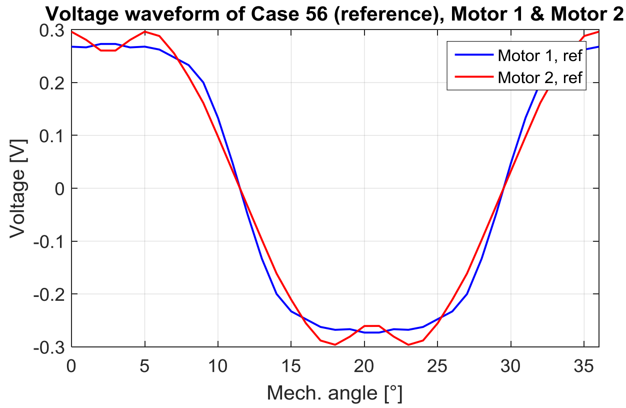

Figure 18

Induced voltage waveform of phase U, @1200 rpm speed, Motor 1 vs. Motor 2

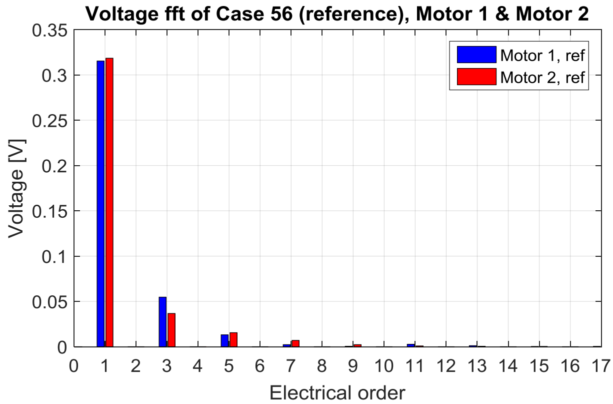

Figure 19

Induced voltage spectrum of phase U, @1200 rpm speed, Motor 1 vs. Motor 2

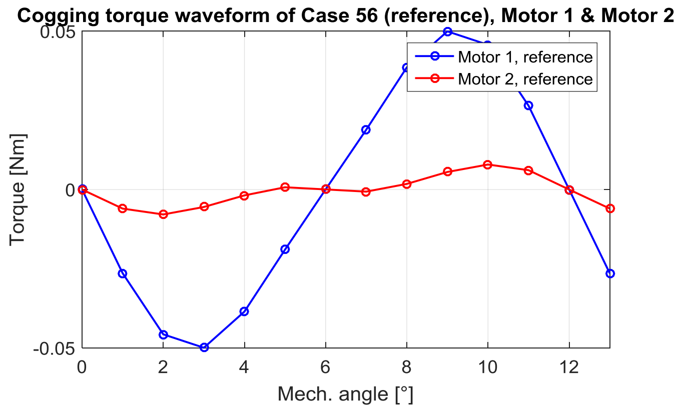

Figure 20

Cogging torque waveform, Motor 1 vs. Motor 2

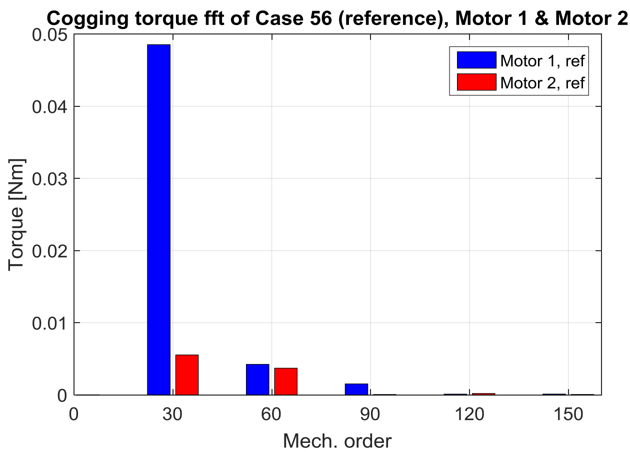

Figure 21

Cogging torque spectrum, Motor 1 vs. Motor 2

Taking a look at the comparison figures it is easy to notice that Motor1 and 2 has almost identical fundamental induced voltage, but the harmonic content is different.

The difference between the motors' cogging torque is even higher. Motor 1 has approximately one magnitude (x10) higher order 30^{th} content while the amount of order 60^{th} is almost the same in Motor 1 and 2.

These differences are the result of the slight modification of the pole shape and will cause the FEM models to have different sensitivity to mesh resolution.

3.2. Sensitivity Results

The sensitivity analysis is run for the cases detailed in Table 2. Figure 22 shows how individual cogging torque orders are changing depending on the mesh resolution corresponding to the case. A converging behaviour of order amplitudes can be noticed.

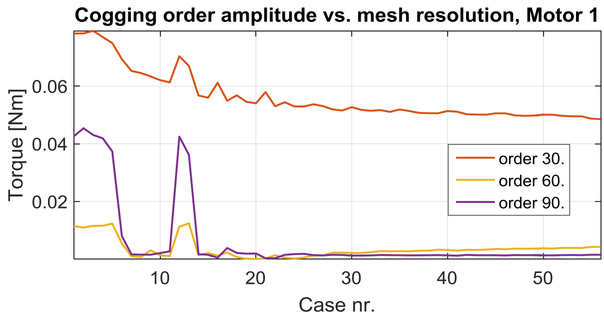

Figure 22

The cogging order amplitudes at each case, Motor 1

Comparing the calculated values to the reference model with the highest resoultion (Case 56) the relative errors are obtained. The relative error is shown in Fig. 23.

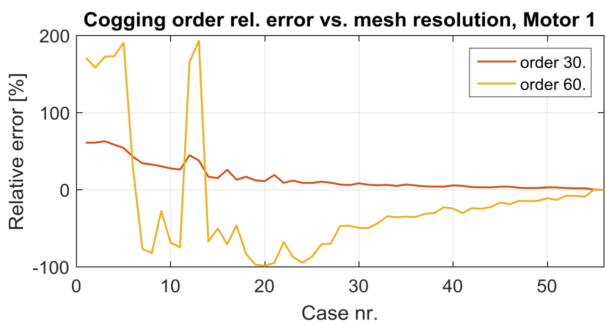

Figure 23

The cogging order amplitudes' relative error at each case, Motor 1

It is worth noticing that the fundamental cogging order (order 30^{th}) reaches a low error (~ 5%) already at case 37^{th} at approx. 11 300 elements, while order 60^{th} converges much slower reaching a below 10% error only at case 52 with approx. 60 000 elements. Therefore relatively high resolution is needed to get precise results with Motor 1. Changes of air gap mesh (changing radial and angular divisions) resolution has a higher effect in the coarsely meshed models (between cases 1 to 20), but all-in-all the global mesh size has the highest effect on the outcome.

Motor 2 however has a different behavior (Fig. 24, 25).

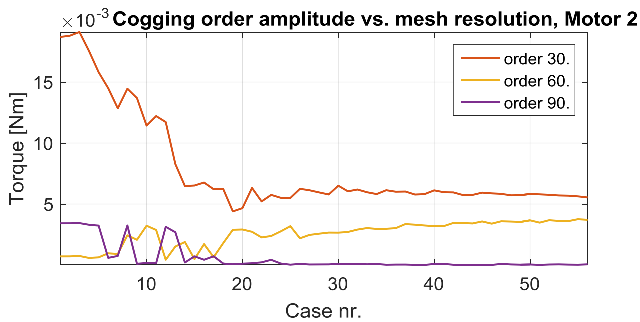

Figure 24

The cogging order amplitudes' relative error at each case, Motor 2

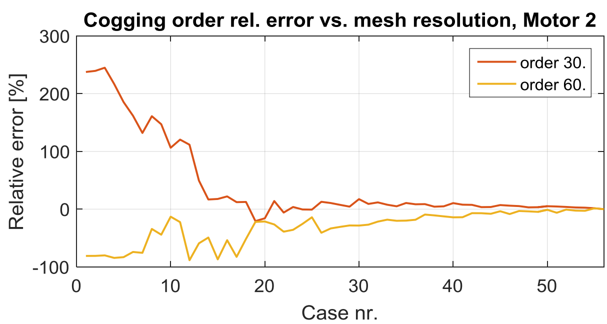

Figure 25

The cogging order amplitudes' relative error at each case, Motor 2

In the case of Motor 2 order 30th and 60th move together in terms of relative error, both reaching a lower than 5% error from case 47 (32 000 elements).

Refinements of air gap mesh has a significant effect on order 30th when the overall mesh is coarse reducing the relative error below 5% at cases 20 to 30 (3 700 to 6 000 elements), however order 60th can only reach a below 10 % error starting from case 37 (11 300 elements).

It should be noted, that in case of Motor 1 the dominant order is order 30th with approx. 10 times higher amplitude than order 60th and the model gives a good results for order 30th already from case 37 (11 300 elements). In case order 60th could be neglected due to its relatively low value, a total of 11 300 elements would be sufficient for the simulation.

Conclusions

The effect of mesh resolution on the calculated cogging torque of permanent magnet synchronous machines was presented using the example of two similar motor models. It was shown how a minor change of geometry can affect a FEM model's sensitivity to the resolution and distribution of the mesh.

It can be concluded that PMSM with an integer slot/pole ratio which have a high cogging torque require a very high mesh density to calculate every harmonic correctly, since lower than required mesh density will result in a false harmonic spectrum (Fig. 25). However in case higher frequency and lower amplitude harmonics can be neglected a relatively coarse mesh might be enough.

On the other hand if the motor design has a low cogging torque a medium to high mesh density might be enough to achieve accurate results and even low resolution mesh variants may represent the harmonics with less errors than in the previous case (Fig. 25).

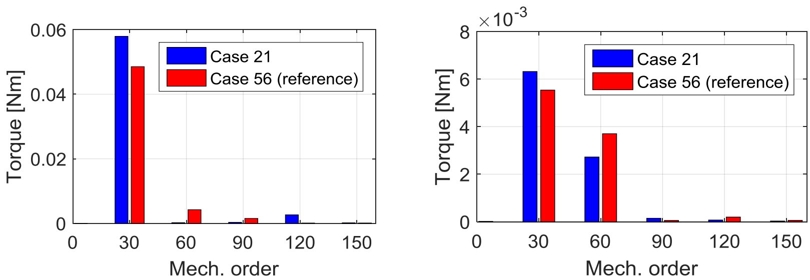

Figure 25

Low vs. very high density mesh, Motor 1 and Motor 2

References

[1] M. Herranz Gracia, K. Hameyer. (2016.07.01). Comparison of numerical methods for the prediction of cogging torque in 2D and 3D, the 13th International Symposiumon Numerical Field Calculation in Electrical Engineering, IGTE 2008, 2008,
Available:
http://134.130.107.200/uploads/bibliotest/2008MHGCogging.pdf

[2] Howe and Z.Q. Zhu, "The influence of finite element discretization on the prediction of cogging torque in permanent magnet excited motors", IEEE Transaction on Magnetics, Vol. 28(2), pp. 1080-1083, March 1992.

[3] A. Arkkio and A. Hannukainen, "Proper finite-element discretization for torque computation of cage induction motors," Power Electronics, Electrical Drives, Automation and Motion (SPEEDAM), 2012 International Symposium on, Sorrento, 2012, pp. 1456-1461. doi: 10.1109/SPEEDAM.2012.6264430

[4] K. Sitapati, "Air-gap layers and adaptive mesh generation for torque calculations in rotating electrical machines," Electrical Machines, 2008. ICEM 2008. 18th International Conference on, Vilamoura, 2008, pp. 1-4. doi: 10.1109/ICELMACH.2008.4799831

[5] B. Silwal, P. Rasilo, L. Perkkiö, A. Hannukainen, T. Eirola and A. Arkkio, "Evaluation and comparison of different numerical computation methods for the electromagnetic torque in electrical machines," Electrical Machines and Systems (ICEMS), 2013 International Conference on, Busan, 2013, pp. 837-842. doi: 10.1109/ICEMS.2013.6713137